Research on Coordinated Optimization of Smart Agriculture Microgrid Configuration and Production Energy Efficiency Driven by Multi-objective Evolutionary Algorithm

Shentong Zhang[1,*], Shuxian Xia[2], Nan Liu[3]
[1]School of Mechanical and Electrical Engineering, Tarim University, Alar 843300, Xinjiang, China
[2]School of Mechanical and Electrical Engineering, Tarim University, Alar 843300, Xinjiang, China
[3]School of Textiles and Apparel, Tarim University, Alar 843300, Xinjiang, China

Corresponding author: Shentong Zhang (e-mail: zst07132026@163.com).

ABSTRACT The smart agriculture park is integrating energy issues into the production process. Electricity is no longer an external input but a continuous condition that maintains the environment for crops. Existing research on microgrids mostly focuses on solving costs, carbon emissions, and reliability, while agricultural loads are often compressed into an exogenous demand curve, making it difficult to identify the transmission of supply shortages to yield and quality. This study establishes a "source-storageload-production" coupled model, placing capacity selection, grid connection boundaries, and agricultural loads in the same code; the target system also examines economic efficiency, emission constraints, supply shortage risks, and production energy efficiency. Based on the results of continuous observations in a smart agriculture park in North China Plain in 2024, the carbon constraint collaborative optimization scheme reduced the total annualized cost by 20.89% compared to the grid benchmark; the carbon emission reduction was 72.18%; unit output energy consumption decreased by 27.23%; production energy efficiency increased by 37.45%, and the critical load guarantee rate reached 99.7%. Compared to five benchmark algorithms, PEC-MOEA achieved higher HV and lower IGD, and had a higher proportion of feasible solutions. The study shows that the core of agricultural microgrid planning is not merely about increasing low-carbon installed capacity, but about integrating energy timing, production tasks, and reliability baselines into the same set of constraints.

INDEX TERMS Smart agriculture; Microgrid; Multi-objective evolutionary algorithm; Energy storage configuration; Low-carbon optimization; Production continuity

I. INTRODUCTION

Electricity has entered the detailed aspects of crop growth and agricultural product circulation. The electrification of agricultural production is not just an increase in the normal load curve. It determines whether the greenhouse can maintain a stable environment, whether irrigation can fall within the appropriate time window, and whether the cold chain can cross the quality risk boundary. Some operations can wait, some environmental control can be slightly shifted, and some loads do not have much room for adjustment. The loss caused by a short-term power outage is not just a few degrees of electricity shortage. Yield, grade, and even the entire production cycle can be affected. Therefore, microgrid planning must simultaneously face two sets of boundaries, one from the power system, and the other from crops and agricultural products. Distributed photovoltaic, wind power, agricultural waste biomass, and batteries provide realistic options for the park's low-carbon energy supply. Existing research has expanded capacity planning from a single cost objective to a cost and carbon emission trade-off [1], and has confirmed that load patterns can change the optimal scale of renewable energy and batteries [2]. The operational conclusions are also clear. Energy storage can increase the consumption of renewable energy, but the benefits depend on capacity and scheduling boundaries [3]; hydrogen energy storage or micro gas turbines and other cross-period resources can also expand the feasible domain [4]. These studies answer how energy equipment is combined, but seldom ask how changes in the energy supply scheme affect production efficiency. Carbon constraints add another layer to the problem. Life cycle studies indicate that carbon performance depends on the capacity structure and also on where the electricity comes from and when it is used [5]. If battery cycle losses are ignored, the benefits of frequent charging and discharging will be overestimated [6]. Off-grid systems also show that improving reliability often requires more energy storage or schedulable backup [7]. Under the influence of electricity prices and resource fluctuations, static optimal solutions may lose long-term feasibility [8]. Even with the same installed capacity, different capacity combinations can still result in different abandoning abilities and supply shortage outcomes [9]. Agricultural microgrids cannot only calculate the proportion of low-carbon electricity but also need to determine whether this electricity supports effective output at the correct time.

Multi-objective evolutionary algorithms are suitable for handling such non-convex, mixed-variable problems. The reference vector method can improve the coverage of the high-dimensional objective space [10]. Energy sharing and demand-side management have expanded the feasible solution set in extreme scenarios [11]. Non-dominated sorting and elite strategies help maintain convergence and diversity [12]. Group intelligence improvement methods have also yielded similar results [13]. However, there is a special requirement for the agricultural scenario. Critical load default cannot be measured with the same yardstick as general cost overruns. Otherwise, a small but serious shortage would be averaged out by the aggregation target. Flexible loads cannot only be shifted based on electricity prices, but the physiological boundaries of crops must be met first. Table 1 contrasts the analysis objects of existing studies with those handled in this paper. The break point of existing studies is here. Capacity planning regards agricultural loads as demands, and agricultural energy efficiency research regards the energy system as inputs. Both are self-consistent, but they do not share the same set of state variables. Thus, capacity models can provide low-cost solutions, but they cannot determine whether this solution misses the irrigation or temperature control windows; production models can explain energy consumption, but rarely answer how much power and energy storage should be configured. This paper places power shortage, load shifting, and production records on the same constraint chain, aiming to repair the explanatory gaps caused by this division.

This article focuses on answering three questions. First, how do agricultural production constraints enter capacity allocation? Second, how do energy storage, biomass, and load flexibility change the trade-off between cost, carbon emissions, and production energy efficiency? Third, how does evolutionary search prioritize the exclusion of

unfeasible solutions in production? These three questions all point to energy allocation under production continuity constraints. Equipment capacity is only the result; the matching of the energy supply sequence and the production tasks is the decision content. The processing path of the research is carried out in three parts: model, algorithm, and verification. At the model level, the production process is no longer explained as a post-event, but enters the energy decision-making through key loads, flexible time windows, and unit output energy consumption. At the algorithm level, PEC-MOEA first ensures production feasibility, then compares the Pareto dominance relationship to avoid cost advantages masking production defaults. At the verification level, progressive scenarios are used to identify the incremental effects of resource access, energy storage configuration, load flexibility, and carbon constraints. The algorithm comparisons and stress tests are used to verify the robustness of the conclusions. The second part presents the theoretical mechanism and research hypotheses. The third and fourth parts give the model and solution methods. The fifth part reports the scenarios and robustness results, and the sixth part discusses the applicable boundaries.

II. THEORETICAL FOUNDATION, MECHANISM AND RESEARCH HYPOTHESES

A. COUPLING LOGIC OF PRODUCTION SYSTEM CONSTRAINTS AND ENERGY INFRASTRUCTURE

Local equipment efficiency cannot directly lead to the performance of the park. The energy system operates based on power balance, marginal cost, and carbon intensity, while agricultural production is constrained by crop stages, operation time limits, and quality risks. The two are connected through loads, and also mutually restrict each other through output and production plans. If agricultural demand is combined into a total load curve, the model will lose the production consequences of load interruptions; if the scarcity of energy is ignored, production plans cannot respond to electricity prices and carbon constraints. The term "synergy" in this article refers to putting these two types of constraints into the same decision space. The value of shared energy storage varies with the service object and consumption mode [14]. In agricultural parks, this value is primarily time transfer. Batteries transfer the excess solar power in the afternoon to the cooling and cold chain periods at night, while biomass provides support during continuous low irradiation or low wind speeds. The difference in purchase and sale electricity prices changes the charging and discharging and grid connection strategies [15], but the price signal cannot cover the production consequences. Electricity in low-price periods that is missed during the irrigation window still has no production value. Production energy efficiency represents the agricultural output formed by unit energy input. It can be improved through energy conservation or reduced through losses. The

former reduces ineffective energy use and supply and demand mismatch, while the latter relies on more stable environmental control to maintain output. Hybrid energy storage helps smooth fluctuating power sources [16], but the electricity saved in one hour cannot directly be explained as an increase in production in the current period. To avoid this short-term attribution, the model calculates production energy efficiency on the planning period scale and uses the constraints of continuous key load and flexible load conservation for the day-ahead scheduling. The mechanism

TABLE 1. Research Streams, Unresolved Issues, and Positioning of This Study

Research stream	Dominant analytical focus	Unresolved issue	Positioning in this study
Microgrid planning	Cost, emissions, reliability and renewable penetration	Agricultural load remains exogenous	Endogenize production constraints and energy productivity
Storage and resilience	Temporal arbitrage, degradation and uncertainty buffering	Critical production consequences are weakly differentiated	Prioritize critical-load continuity and hierarchical feasibility
Agrivoltaics and food-energy systems	Land, light, crop yield and renewable co-production	Limited linkage to microgrid capacity and dispatch	Connect agronomic flexibility with source-storage sizing
Multi-objective evolutionary optimization	Pareto convergence, diversity and computational efficiency	Feasible solutions may violate production logic	Embed production-aware repair and compromise selection

can be observed in two steps. The power side changes first. Energy storage and dispatchable units reduce the gap between supply and demand, and flexible loads increase the utilization of local renewable energy. The production side then responds. The greenhouse environment and cold chain status become more stable, incomplete operations decrease, and unit output energy consumption changes accordingly. If the first step improves but the second step does not respond, the configuration optimization can only be called an improvement in energy efficiency, not an improvement in production energy efficiency. This article also reports the key load guarantee rate, annual output, and unit output energy consumption to test whether these two steps occur simultaneously.

B. SOURCE-STORAGE COMPLEMENTARITY, RELIABILITY BUFFERING AND LOW-CARBON PERFORMANCE

Renewable energy first changes the supply structure, but reliability may not necessarily improve. Solar power has a stable day-night cycle, while wind power is more random in its fluctuations; cooling and cold chain during the night and throughout the day are not synchronized with the two. Without energy storage, the loss of power during the afternoon and the purchase of electricity at night may occur simultaneously. The multi-microgrid research has incorporated resource relevance and load deviation into scenario generation [17], and the hybrid battery-hydro energy storage also shows the value of cross-time-scale buffering [18]. This study retains the biomass unit to undertake continuous support, while limiting its fuel and emission boundaries. Thus, various resources on the supply side are no longer simply added together but share tasks according to the time scale. Carbon constraints change the power supply structure and also the operation sequence. More agricultural tasks will be moved to the windows with sufficient low-carbon electricity. As long as the migration is within the temperature and humidity, soil moisture, and operation time limits, costs, carbon emissions, and energy efficiency can be improved in the same direction. Beyond the agronomic boundaries, emission reduction benefits will be transformed into production risks. Based on this distinction, H1 and H2 are proposed. This transmission chain also provides counterexample conditions. If S1 can still maintain critical load support without energy storage, then time buffering is not necessary; if LPSP does not decrease after adding batteries to S2, the connection between energy storage and reliability does not hold; if the combined pressure scenario leads to a rapid crossing of supply shortage, the complementarity of biomass and batteries can only explain normal operation. Therefore, H1 and H2 do not rely on a single optimal value but must simultaneously accept the tests of adjacent scenarios and pressure scenarios.

H1: Compared with the grid benchmark and the scheme only configured with renewable energy, the "source-storage-load-production" collaborative optimization, after introducing energy storage, dispatchable biomass, and flexible agricultural load, can reduce unit output energy consumption and improve production efficiency while maintaining critical load guarantee.

H2: There is reliability complementarity between energy storage and dispatchable biomass, and this complementarity can inhibit the transmission of renewable energy deviations to LPSP and critical load default, and improve the feasibility of the scheme under combined disturbances.

C. PRODUCTION EFFICIENCY MECHANISM

Whether agricultural loads are adjustable depends on the task itself. Irrigation can be shifted within the allowable range of soil moisture; cold chain and basic environment control are close to rigid, and the interruption cost is much higher than ordinary load deviations. Cooling, ventilation, and supplementary lighting are between the two, and the adjustable space comes from the environmental allowable range. Research on agricultural photovoltaic systems has proved that shading, light, and energy benefits must be evaluated together with the crop response [19]. The coupled system of water, food, and energy has reached the same understanding [20], and the rice agricultural photovoltaic model also shows that energy output is constrained by crop yield [21]. Therefore, agricultural flexibility is not a demand response capacity that can be called upon at any time. It is a production choice with a time window and cost. The target weights will change the spatial layout and resource allocation of the agricultural photovoltaic system [22], and the improvement of the light environment may not correspond to the optimal overall output [23]. Based on this, this paper sets an upper limit for the proportion of flexibility and requires that the energy moved in and out during the scheduling period be equal. This constraint is very important. It allows the load to follow renewable energy but does not allow the model to achieve "energy saving" by not completing irrigation or temperature control tasks. When approaching the agronomic upper limit, production risks increase, and the available space for additional flexibility narrows.

H3: Under the constraints of energy conservation and agronomic boundaries, the time shift of agricultural production loads can increase renewable energy consumption and reduce system costs, and its improvement of production efficiency is regulated by the total load size and carbon constraints.

D. CONSTRAINT-AWARE EVOLUTIONARY SEARCH AND IMPLEMENTABILITY

Multi-objective evolutionary algorithms can provide a set of compromise solutions suitable for non-convex capacity planning. Relevant reviews have included battery, hydrogen energy storage, and various heuristic algorithms for comparison, but constraint handling and repeatable evaluation remain weak links [24]. Research on DC microgrids under uncertainty also reaches similar conclusions [25]. Agricultural loads further increase the level of constraints. Critical load interruption belongs to production default, SOC boundary crossing belongs to physical default, and non-conservation of flexible loads means that tasks are deleted. Combining these three into the same penalty coefficient makes the search direction prone to distortion. PEC-MOEA repairs individuals based on the consequences of default. First, restore the critical loads and power balance, then handle the SOC and equipment boundaries, and subsequently correct the conservation of flexible loads. Only the feasible individuals will enter the elite archive according to the non-dominated relationship and crowding degree. The calculation time will increase, but the iterations occupied by the ineffective individuals will decrease. H4 then examines whether this repair sequence can improve the coverage of the effective frontier.

H4: Compared with the benchmark multi-objective algorithm that uses general constraints, the production constraint-aware repair and feasibility priority strategy can increase the proportion of feasible solutions, and simultaneously improve the HV, IGD, and distribution quality of the solution set. Table 2 lists the four hypotheses, comparison scenarios, and evaluation indicators.

III. SYSTEM BOUNDARY, DATA FOUNDATION AND MATHEMATICAL MODEL

A. RESEARCH OBJECT

The case park is located in the warm temperate monsoon zone of the central part of the North China Plain. The name, administrative region and coordinates of the park have been anonymized due to business confidentiality requirements. The continuous observation period is from January 1, 2024 to December 31, 2024. All timestamps are unified as China standard time. Power, meteorological and production records are summarized at a 15-minute interval; the annual records are used for capacity and performance accounting. The connection point, distributed power sources and main load branches use 0.5S class smart meters, with an energy resolution of 0.01 kWh. The irradiance record resolution is 1 W/m^2, with an uncertainty not exceeding 2%; the wind speed resolution is 0.1 m/s, with a measurement error not exceeding 0.3 m/s. The temperature and relative humidity resolution is 0.1 °C and 0.1%RH respectively, with an error not exceeding 0.3 °C and 2%RH. The output is taken from the batch production ledger of the park and is verified monthly. The planning boundary covers asset investment, annual operation and intraday power balance. The migratable operations mainly come from irrigation and some temperature control, while the cold chain and basic environmental control are treated as critical loads. Data cleaning is carried out according to the pre-set unified rules. Isolated missing or gaps of no more than 1 hour in a row are interpolated linearly; longer gaps are filled with the median of the same moment in the previous 7 days. Outliers are identified using a 7-point Hampel window, with the threshold set as the absolute deviation of 3 medians, and then checked for daily energy conservation after correction. The power and meteorological sequences are connected by timestamp, and the production ledger is summarized monthly and matched with the energy consumption records. Missing and corrected records do not participate in the calculation of algorithm performance indicators. This park has both fluctuating power sources and dispatchable units, and has the conditions for energy storage access. The agricultural load covers migratable operations and rigid guarantee requirements, making it suitable for observing the conflict between supply fluctuations and production continuity. It is not a statistical representative sample of the agricultural parks in North China. The 15- minute resolution retains the photovoltaic ramp, irrigation start-stop and temperature control fluctuations at the planning scale, and avoids bringing second-level control noise into the capacity model. This aggregation smooths short-term peaks, so the critical load constraints are still checked against the original branch records, and cannot rely solely on the aggregation curve. Interpolated data is only used to fill the annual energy sequence; dates with continuous long gaps do not participate in the selection of representative days. Sensitivity and stress scenarios are based on the cleaned benchmark sequence, with unified application of resource, load and price deviations. This can distinguish between measurement gaps and planning uncertainties. The capacity accounting for each season within the year still uses all qualified periods and does not replace the annual energy balance with representative days.

TABLE 2. Theoretical Hypotheses and Empirical Operationalization

Hypothesis	Mechanism	Operational comparison	Primary indicators
H1	Source-storage-load-production coordination	S2–S4 versus S0–S1	UEC, PEE, critical-load satisfaction
H2	Storage-dispatchable generation reliability complementarity	S1 versus S2 and U0–U9	LPSP, feasibility status, emissions
H3	Agronomically bounded load shifting	S2 versus S3–S4 and sensitivity shocks	Renewable penetration, cost, PEE
H4	Production-aware constraint repair	PEC-MOEA versus five benchmarks	HV, IGD, spacing, feasible ratio

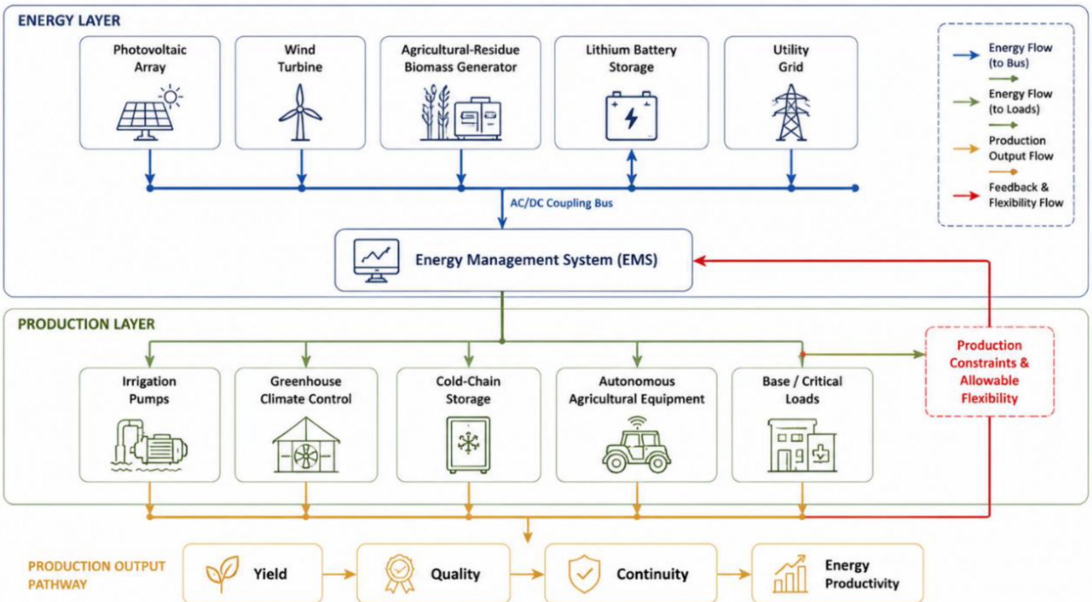

FIGURE 1. Source-Storage-Load-Production Coupled Architecture of the Smart Agricultural Microgrid

B. PROGRESSIVE PRESENTATION OF DECISION VARIABLES, PARAMETERS AND SCENARIOS

The decision vector includes supply capacity, energy storage scale, grid connection boundary, and production flexibility. The eight variables are shown in Table 3. Photovoltaic and wind power provide the upper limit of fluctuating supply, biomass offers dispatchable output, and batteries undertake time transfer. Inverters and grid connection capacity limit energy exchange. Irrigation and greenhouse flexibility determine the peak-shifting space on the production side. Capacity and flexibility are encoded in the same chromosome, avoiding the situation where equipment is predetermined first and then the load is passively adjusted.

Table 4 lists the technical and economic parameters used in the model. The battery's round-trip efficiency is 90%, and the operating range of the SOC is 15% - 95%; the difference between the purchase and sale electricity prices is used to limit grid-connected arbitrage, and the emission factors of the power grid and biomass are included in the carbon accounting. The minimum satisfaction rate of the critical load is set at 98.5%. Schemes below this threshold can be retained as diagnostic scenarios but will not be included in the final candidate set.

Mechanisms S0-S4 are gradually added according to Table 5. S0 is the grid benchmark. S1 increases renewable energy but without batteries, to observe the benefits and risks of the expansion of installed capacity itself. S2 adds energy storage, S3 further opens the flexibility of agricultural loads, and S4 imposes carbon constraints and optimizes production energy efficiency. The adjacent scenarios only change limited conditions to facilitate tracking the source of results. The critical load guarantee rate of S1 is lower than 98.5%, so it is only used for diagnostic comparison.

C. MULTI-OBJECTIVE FUNCTION

The total annualized cost includes capital annualization, operation and maintenance, replacement, net purchase and sale of electricity from the grid. The capital recovery factor is determined by the discount rate r and the equipment life n_i, and assets with different lifetimes are thus included in the same annual scale. This approach continues the annualized accounting method in the cost-carbon emission joint planning [1]:

$$\min f_1(x) = \sum_{i\in\Omega} C_i^{\mathrm{cap}} x_i \frac{r(1+r)^{n_i}}{(1+r)^{n_i}-1} + C^{\mathrm{om}} + C^{\mathrm{rep}} + \sum_{t=1}^{T}\left(c_t^{\mathrm{buy}}P_t^{\mathrm{buy}} - c_t^{\mathrm{sell}}P_t^{\mathrm{sell}}\right)\Delta t \tag{1}$$

Carbon target accounting equates the emissions during

TABLE 3. Decision Variables and Feasible Domains

Variable	Description	Unit	Lower	Upper	Role
PV_CAP	PV installed capacity	kW	0	1200	Determines solar generation potential
WT_CAP	Wind turbine capacity	kW	0	500	Complements PV generation
BIO_CAP	Biomass generator capacity	kW	0	250	Dispatchable low-carbon backup
BESS_CAP	Battery energy capacity	kWh	0	2000	Buffers renewable variability
INV_CAP	Inverter capacity	kW	0	1200	Limits conversion capability
FLEX_IRR	Flexible irrigation scheduling ratio	%	0	35	Represents movable irrigation load
FLEX_GH	Greenhouse climate-control flexibility	%	0	18	Constrained by crop environment requirements
GRID_MAX	Maximum grid exchange power	kW	0	600	Limits import/export capacity

TABLE 4. Selected Technical and Economic Parameters

Component	Parameter	Unit	Value
PV array	Capital cost	USD/kW	690
Wind turbine	Capital cost	USD/kW	1220
Biomass generator	Capital cost	USD/kW	2050
Battery storage	Capital cost	USD/kWh	185
Battery storage	Round-trip efficiency	%	90
Battery storage	SOC lower bound	%	15
Battery storage	SOC upper bound	%	95
Grid electricity	Purchase tariff	USD/kWh	0.142
Grid electricity	Feed-in tariff	USD/kWh	0.056
Emission factor	Grid	kgCO2/kWh	0.581
Emission factor	Biomass	kgCO2/kWh	0.092
Agricultural production	Annual yield baseline	t/year	842
Agricultural production	Critical load minimum satisfaction	%	98.5

TABLE 5. Scenario Design and Incremental Mechanisms

Scenario	Configuration logic	Renewable	Battery	Production flexibility	Carbon constraint
S0	Grid-only baseline	No	No	No	No
S1	Renewable generation only	Yes	No	No	No
S2	Renewable-storage coordination	Yes	Yes	No	No
S3	Production-load flexibility	Yes	Yes	Yes	No
S4	Carbon-constrained co-optimization	Yes	Yes	Yes	Yes

the operation period of grid power purchase and biomass power generation. The equipment manufacturing stage is not included in the current data scope; after obtaining a complete life cycle list, the embodied carbon can be added to the same target:

$$\min f_2(x) = \sum_{t=1}^{T} \left(EF_{\text{grid}} P_t^{\text{buy}} + EF_{\text{bio}} P_t^{\text{bio}} \right) \Delta t \tag{2}$$

The LPSP describes overall supply deficiency, but it will dilute the significant but relatively small critical load gap. Therefore, the model sets a hard constraint on the critical load satisfaction rate. The former is used to compare overall reliability, while the latter ensures the production bottom line:

$$\min f_3(x) = \text{LPSP} = \frac{\sum_{t=1}^{T} E_t^{\text{unserved}}}{\sum_{t=1}^{T} E_t^{\text{load}}} \tag{3}$$

The production energy efficiency (PEE) is defined as the ratio of the effective output (Y) to the agricultural energy consumption. The unit output energy consumption (UEC) provides the reciprocal expression. These two indicators report the same efficiency fact from different perspectives and should not be counted separately as independent results:

$$\max f_4(x) = \text{PEE} = \frac{10^3 Y}{\sum_{t=1}^{T} E_t^{\text{agri}}} \tag{5}$$

$$\text{UEC} = \frac{\sum_{t=1}^{T} E_t^{\text{agri}}}{Y} \tag{6}$$

The four objectives cannot be added up a priori. Low cost may rely on more grid power purchases, deep emission reduction may require additional investment, and reliability is usually accompanied by capacity redundancy. Production energy efficiency is also affected by both production volume and energy consumption. In the search stage, no weights are preset; instead, a Pareto set is formed first, and then a compromise solution is selected.

D. OPERATIONAL CONSTRAINTS AND PRODUCTION CONSTRAINTS

The supply and demand at any given time must satisfy the power balance. The supply comes from distributed power sources, energy storage discharge, and grid power purchases; the demand consists of agricultural electricity consumption, energy storage charging, external power transmission, and unmet loads:

$$P_t^{\mathrm{pv}} + P_t^{\mathrm{wt}} + P_t^{\mathrm{bio}} + P_t^{\mathrm{dis}} + P_t^{\mathrm{buy}} + P_t^{\mathrm{unserved}} = P_t^{\mathrm{agri}} + P_t^{\mathrm{ch}} + P_t^{\mathrm{sell}}, \qquad \forall t \tag{7}$$

The energy storage state evolves continuously based on charging and discharging efficiency and is subject to capacity proportion boundary constraints. To prevent simultaneous charging and discharging in the same period, the charging and discharging state variables satisfy mutually exclusive conditions; the impact of battery degradation on the scheduling value has been proven by relevant studies [6]. In this paper, within the allowable range of data, this impact is absorbed by annualized replacement costs:

$$\begin{gathered} \mathrm{SOC}_t = \mathrm{SOC}_{t-1} + \frac{\eta_{\mathrm{ch}} P_t^{\mathrm{ch}} \Delta t}{E^{\mathrm{bess}}} - \frac{P_t^{\mathrm{dis}} \Delta t}{\eta_{\mathrm{dis}} E^{\mathrm{bess}}}, \\ \mathrm{SOC}^{\min} \le \mathrm{SOC}_t \le \mathrm{SOC}^{\max} \end{gathered} \tag{8}$$

$$\begin{aligned} &0 \le P_t^{\mathrm{ch}} \le u_t P_{\mathrm{ch}}^{\max}, \\ &0 \le P_t^{\mathrm{dis}} \le (1-u_t) P_{\mathrm{dis}}^{\max}, \qquad u_t \in \{0,1\} \end{aligned} \tag{9}$$

The agricultural flexible load consists of the baseline load and the migration quantity. During the scheduling period, the energy that is moved in and the energy that is moved out must be equal, and the deviation amplitude must not exceed the agronomic upper limit. Therefore, the model cannot reduce costs by permanently reducing irrigation or temperature control tasks:

$$\begin{gathered} P_{k,t}^{\mathrm{flex}} = P_{k,t}^{\mathrm{base}} + \Delta P_{k,t}, \\ \sum_{t \in T_k} \Delta P_{k,t} \Delta t = 0, \\ |\Delta P_{k,t}| \le \phi_k P_{k,t}^{\mathrm{base}} \end{gathered} \tag{10}$$

The satisfaction rate of the key load set Ωc must not be lower than αc. The equipment output, grid connection exchange, and utilization of renewable energy are also subject to their respective capacity constraints. The hard constraints are carried out in parallel with LPSP to avoid the average reliability masking production default:

$$\begin{gathered} \mathrm{CSR}_c = 1 - \frac{\sum_t E_{c,t}^{\mathrm{unserved}}}{\sum_t E_{c,t}^{\mathrm{demand}}} \\ \ge \alpha_c = 0.985, \qquad \forall c \in \Omega_c \end{gathered} \tag{11}$$

$$\begin{gathered} 0 \le P_t^j \le \overline{P^j}(x), \\ \left| P_t^{\mathrm{buy}} - P_t^{\mathrm{sell}} \right| \le P^{\mathrm{grid,max}}, \qquad j \in \{\mathrm{pv}, \mathrm{wt}, \mathrm{bio}\} \end{gathered} \tag{12}$$

IV. PEC-MOEA SOLUTION METHOD AND EXPERIMENTAL DESIGN

A. ENCODING, EVALUATION, AND PRODUCTION CONSTRAINT SENSITIVITY RESTORATION

PEC-MOEA encodes eight planning variables with real number chromosomes. The inner scheduling is used to calculate the violation amount of the four objectives and constraints. Reference vectors and multi-strategy search help cover the high-dimensional objective space [10], but the ordinary penalty function cannot distinguish the consequences of default. This paper divides feasibility into three layers. The first layer corresponds to critical loads and power balance, the second layer corresponds to SOC and equipment boundaries, and the third layer corresponds to the conservation of flexible loads. Costs and carbon preferences only participate in ranking after the first three layers are feasible. Restoration starts from the production bottom line. The algorithm first calls for compensating the key load gap with available resources, then adjusts charging and discharging to bring SOC back to the feasible range, and finally restores the conservation of flexible loads according to the time window. Individuals that still violate the key constraints cannot enter the elite archive, even if they are outstanding in a certain objective. This reduces the search time spent in physically infeasible areas and makes the algorithm evaluation closer to the real operation rules. The solution process is shown in Figure 2. After encoding and evaluation of the four objectives, the algorithm performs hierarchical restoration, followed by non-dominated sorting, crowding degree control, and elite update. After reaching the termination generation, the feasible Pareto archive is retained, and a compromise solution is selected according to the decision preference. The constraint levels in the figure are the algorithm structures tested by H4.

B. PARETO SORTING AND TRADE-OFF SOLUTION SELECTION

The four objectives have different dimensions and directions, and need to be normalized before entering the trade-off selection process. For the minimization objective, the interval positive scaling is adopted, while for the maximization of production energy efficiency, it is converted into the loss from the ideal value. If the optimal and worst values of the m-th objective in the Pareto set are f_m^* and f_m^-, the normalized loss is:

$$z_m(x) = \begin{cases} \dfrac{f_m(x) - f_m^*}{f_m^- - f_m^*}, & m \in M_{\min}, \\ \dfrac{f_m^* - f_m(x)}{f_m^* - f_m^-}, & m \in M_{\max} \end{cases} \tag{13}$$

The compromise solution employs the weighted Lp distance. The baseline result assigns equal weights to the four objectives, avoiding pre-determined conclusions before the search is completed. The operator can also modify the weights based on capital, carbon constraints, and crop risks.

$$\begin{gathered} x^c = \arg\min_{x \in P} \left[\sum_{m=1}^{4} w_m z_m(x)^p \right]^{1/p}, \\ \sum_{m=1}^{4} w_m = 1, \qquad p = 2 \end{gathered} \tag{14}$$

The algorithm comparison report includes HV, IGD, Spacing, Spread, the proportion of feasible solutions, and running time. The larger the HV, the better; the smaller the

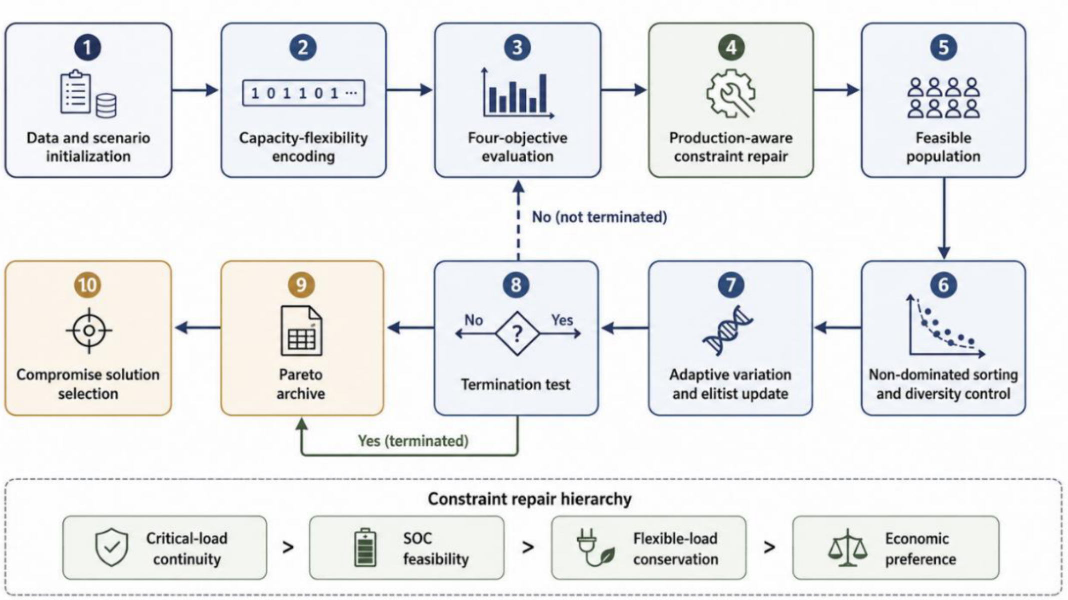

FIGURE 2. Production-Energy Coupled Multi-Objective Evolutionary Optimization Workflow

IGD, the better. Spacing and Spread measure the distribution of the solution set. The proportion of feasible solutions reflects how much of the computational budget actually enters the production implementable area. Running time is compared only under the same hardware and single-process environment.

C. TEST STRATEGY

The benchmark group consists of five commonly used algorithms. NSGA-II and NSGA-III respectively represent non-dominated sorting and reference vector thinking; MOEA/D adopts a decomposition framework, MOPSO adopts particle swarm update, and SPEA2 adopts strength Pareto evaluation. The six algorithms use the same objectives, constraints, population size, and termination generations. The test begins with the mechanism comparison from S0 to S4, then proceeds to frontier quality evaluation, parameter perturbation, and U0-U9 composite scenarios. This allows for the separation of mechanism differences, search differences, and external disturbances. All algorithms run independently 30 times with a population size of 200 and a maximum iteration generation of 300. The random seed is fixed sequentially as 202401-202430. PECMOEA uses simulated binary crossover and polynomial mutation: crossover probability 0.90, crossover distribution index 20; mutation probability 1/8, mutation distribution index 20. The upper limit of the elite archive is 200. The six algorithms are executed in the same Python environment, on the same workstation, and in a single-process mode. HV, IGD, Spacing, and Spread are reported as the average and standard deviation of 30 runs. The fairness of comparison also depends on the reference frontier and the computational budget. All six algorithms use a 200 x 300 individual evaluation budget, without additional calculations due to premature convergence. The reference point for HV is determined by expanding the worst value of the objectives from all 30 runs by 5%; the reference set for IGD takes the non-dominated set after merging all run results. Each objective is normalized by the reference set range first, and then the distance and volume indicators are calculated. The same random seed is used for the same sequence of runs to reduce the interference of resource scenario sampling differences on algorithm sorting.

V. RESULT ANALYSIS

A. DAILY SUPPLY AND DEMAND STRUCTURE AND MULTI-OBJECTIVE TRADE-OFF

Figure 3 first presents the daily supply and demand structure. Greenhouse control and cold chain form the base of the daily load, irrigation shows local high values in the morning and evening, and intelligent equipment mainly operates during the day. Solar power rises rapidly after 7 o'clock, and the output at noon exceeds the load during the same period; wind power is relatively gentle, but it is not sufficient to independently meet the demand at night. Biomass fills the gap in the early morning and evening. Without energy storage and load migration, the surplus at noon and the gap at night will exist simultaneously. The reliability of S1 can thus be explained from the daily curve.

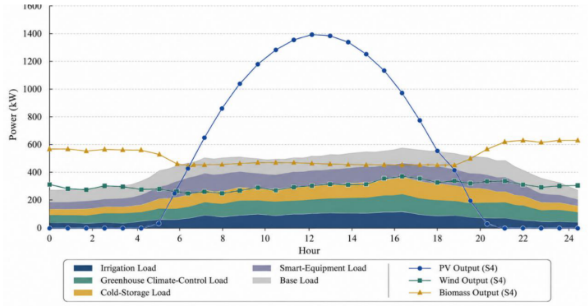

FIGURE 3. Agricultural Load Composition and Distributed Generation Profile under S4

The 108 Pareto samples are clearly depicted as a cost-carbon emission slope in Figure 4. The low-cost solutions typically retain more electricity purchases or less energy storage, while the low-emission solutions require additional renewable energy and buffer capacity. The PEC-MOEA retains more continuous feasible solutions in the medium and low emission areas.

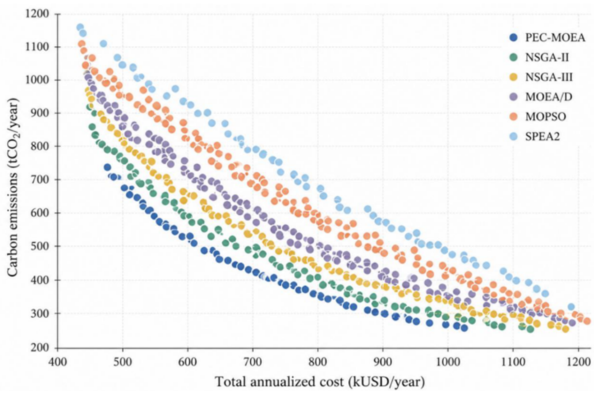

FIGURE 4. Pareto Solution Distribution for Economic and Carbon Objectives

B. EVOLUTION OF CAPACITY CONFIGURATION STRUCTURE

The capacity results for the five scenarios are shown in Table 6. In S1, 620 kW of photovoltaic, 120 kW of wind power, and 80 kW of biomass are installed, but no batteries are included. In S2, after adding 1150 kWh of energy storage, the capacities of the three types of power sources continue to increase, and the upper limit of grid connection exchange decreases from 430 kW to 360 kW. In S3, the flexible load is opened, and the adjustable proportions of irrigation and greenhouses increase to 22% and 11% respectively. In S4, the final configuration is 910 kW of photovoltaic, 240 kW of wind power, 120 kW of biomass, and 1550 kWh of batteries. Deep emission reduction relies on the expansion of fluctuating power sources and time buffers together.

Figure 5 shows that after S2, the component with the fastest growth was battery capacity. The biomass growth was relatively small, serving as a supporting role during periods of low resources rather than being the main energy provider. From S3 to S4, the total annualized cost increased from 252.7 to 259.8 kUSD/year, with an increase of 2.81%; during the same period, carbon emissions decreased from 620 to 468 tCO2/year. The cost increase corresponds to stricter emission reduction requirements, not a failure in the configuration.

C. SYNERGISTIC RESULTS OF ECONOMY, ENVIRONMENT, RELIABILITY AND PRODUCTION ENERGY EFFICIENCY

Table 7 exposes the flaws of S1. Compared with S0, S1 reduces the cost from 328.4 to 287.6 kUSD/year, and the carbon emission from 1682 to 1105 tCO2/year; however, the LPSP increases from 0.004 to 0.027, and the critical load guarantee rate drops to 97.9%, which is lower than the baseline of 98.5%. The improvement in average cost and emissions cannot offset the temporal mismatch. After adding batteries to S2, the LPSP drops to 0.010, the critical load guarantee rate rises to 99.2%, and the unit output energy consumption drops to 338 kWh/t. This set of adjacent scenarios provides the first piece of evidence for H2. After opening production flexibility in S3, the total annualized cost drops to 252.7 kUSD/year, the lowest among all five scenarios; the penetration rate of renewable energy is 68.4%, and the PEE is 3.15 kg/kWh. S4 continues to impose carbon constraints. The cost is 2.81% higher than S3, but the carbon emission drops by 24.52%, the LPSP drops to 0.006,

the PEE rises to 3.23 kg/kWh, and the critical load guarantee rate reaches 99.7%. The lowest cost solution is different from the comprehensive compromise solution. Changes at the production end do not come solely from compressing loads. The annual output from S0 to S4 increases from 842 to 858 t/year, and the unit output energy consumption drops from 426 to 310 kWh/t. Total energy consumption decreases while effective output increases simultaneously. If only PEE is reported, the two sources will be combined; listing both output and UEC together shows that the improvement comes from both energy supply timing optimization and reduction of critical operations.

When the table is converted to a relative scale, this difference becomes even clearer. Compared with S0, S4 reduces costs by 20.89%, cuts carbon emissions by 72.18%, and reduces unit output energy consumption by 27.23%, while PEE increases by 37.45%. The comprehensive improvement index is 50.18%. S3 has a greater cost reduction, and S4 has a higher comprehensive improvement. Operators need to clearly define the carbon constraints and production risk preferences between the two.

D. ALGORITHM PERFORMANCE

Table 9 presents the mean and standard deviation of 30 independent runs. The HV of PEC-MOEA is 0.827, which is 6.30% higher than that of the suboptimal NSGA-III; the IGD is 0.041, which is 29.31% lower; the proportion of feasible solutions is 98.6%, which is 5.5 percentage points higher. Spacing and Spread are also in the optimal direction. However, the cost is an increase in running time to 142

TABLE 6. Optimal Capacity and Production-Flexibility Configuration

Scenario	PV (kW)	Wind (kW)	Biomass (kW)	Battery (kWh)	Grid limit (kW)	Irrigation flex. (%)	Greenhouse flex. (%)
S0	0	0	0	0	520	0	0
S1	620	120	80	0	430	0	0
S2	780	180	100	1150	360	8	4
S3	850	220	100	1320	330	22	11
S4	910	240	120	1550	305	26	14

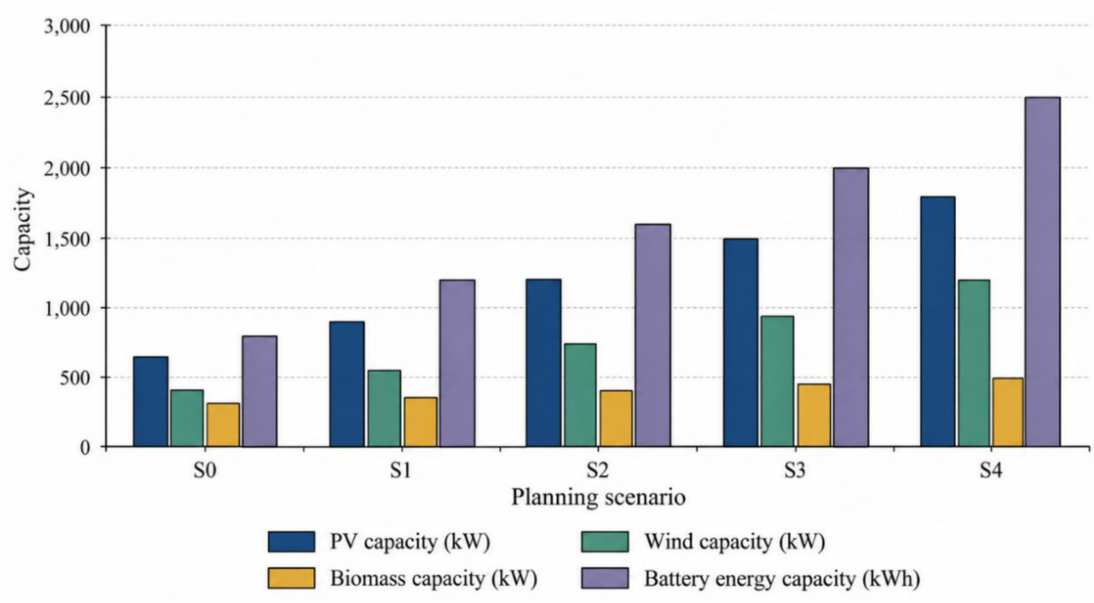

FIGURE 5. Optimal Capacity Configuration across Planning Scenarios

TABLE 7. Economic, Environmental, Reliability and Production-Energy Performance

Scenario	TAC (kUSD/y)	LCOE (USD/kWh)	CO2 (t/y)	RE (%)	LPSP	UEC (kWh/t)	PEE (kg/kWh)	Critical load (%)
S0	328.4	0.172	1682	0.0	0.004	426	2.35	98.8
S1	287.6	0.151	1105	42.1	0.027	383	2.61	97.9
S2	269.2	0.142	714	63.5	0.010	338	2.96	99.2
S3	252.7	0.133	620	68.4	0.007	317	3.15	99.5
S4	259.8	0.137	468	75.2	0.006	310	3.23	99.7

TABLE 8. Relative Performance Improvement against the S0 Baseline

Scenario	Cost reduction (%)	Carbon reduction (%)	UEC reduction (%)	PEE increase (%)	Composite improvement (%)
S0	0.00	0.00	0.00	0.00	0.00
S1	12.42	34.30	10.09	11.06	22.58
S2	18.03	57.55	20.66	25.96	38.47
S3	23.05	63.14	25.59	34.04	43.52
S4	20.89	72.18	27.23	37.45	50.18

seconds, while NSGA-II and MOPSO are 118 seconds and 109 seconds respectively. For capacity planning, this time increment is exchanged for more feasible solutions and better frontier coverage.

Figure 6 only retains three complementary indicators: HV, IGD, and the proportion of feasible solutions. PEC-MOEA is superior simultaneously in all three directions. When the feasibility rate increases, HV and IGD do not deteriorate, and hierarchical repair does not compress the search to a small number of conservative solutions. H4 receives descriptive support.

E. PARAMETER SENSITIVITY AND MARGINAL RESPONSE

Table 10 uniformly examines a +20% shock. The increase in grid electricity prices leads to a 4.60% increase in the total annualized cost; the increase in battery costs results in a 3.00% increase in cost, a 0.79% increase in carbon

TABLE 9. Comparative Performance of Multi-Objective Optimization Algorithms

Algorithm	HV mean ± SD	IGD mean ± SD	Spacing	Spread	Feasible ratio (%)	Runtime (s)
PEC-MOEA	0.827 ± 0.018	0.041 ± 0.006	0.026	0.329	98.6	142
NSGA-II	0.761 ± 0.027	0.064 ± 0.011	0.039	0.402	91.8	118
NSGA-III	0.778 ± 0.024	0.058 ± 0.010	0.036	0.381	93.1	136
MOEA/D	0.744 ± 0.031	0.071 ± 0.014	0.043	0.417	89.7	126
MOPSO	0.711 ± 0.038	0.083 ± 0.016	0.052	0.455	86.3	109
SPEA2	0.735 ± 0.034	0.076 ± 0.013	0.047	0.431	88.9	131

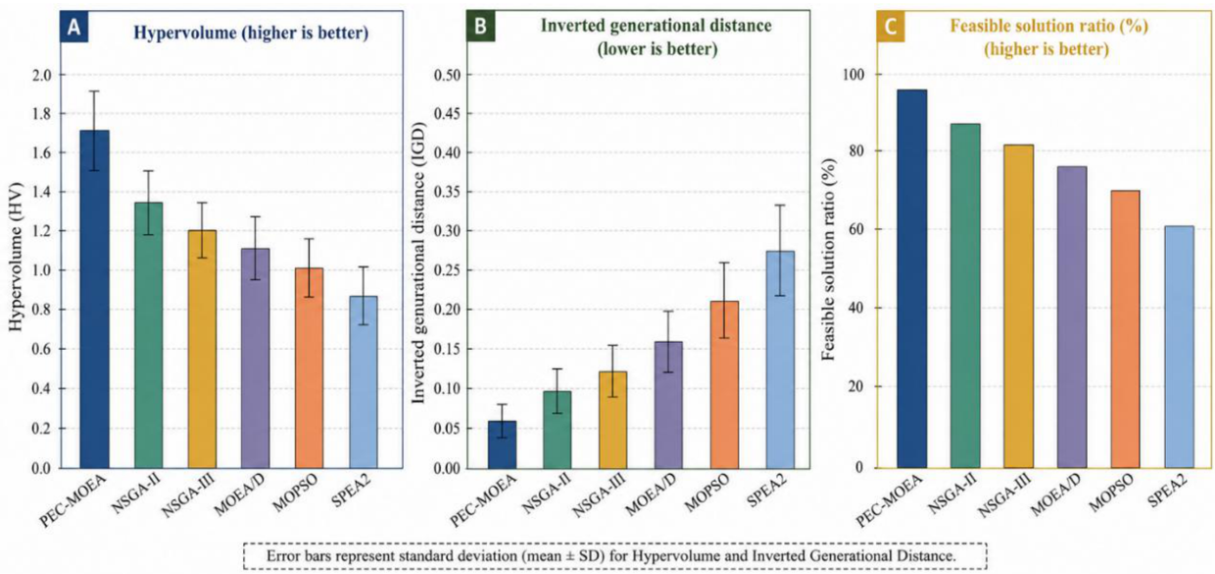

FIGURE 6. Comparative Algorithm Performance in Convergence and Feasibility

emissions, and a 0.59% decrease in PEE. The grid emission factor mainly affects the carbon assessment: after the factor increases by 20%, carbon emissions increase by 6.20%, while the cost only changes by 0.40%. When production increases by 20%, PEE increases by 11.61%; when agricultural load increases by 20%, the cost and carbon emissions increase by 3.60% and 2.61% respectively, and PEE decreases by 3.19%. Cash flow risk mainly comes from electricity prices, while energy productivity is more affected by production and total load.

Figure 7 presents the complete trajectory from -20% to +20%. The cost slopes of electricity price and agricultural load growth are the highest, followed by battery costs, and then photovoltaic costs. The direct impact of production output and grid emission factors on costs is very small. The cost sensitivity does not overlap with the production energy efficiency sensitivity. Load flexibility can change the timing, but it cannot eliminate the capacity pressure caused by the continuous growth of total demand. The applicable range of H3 ends here.

F. COMPOSITE UNCERTAINTY AND PRESSURE FEASIBILITY

Composite disturbances are closer to planning risks than single-factor changes. Relevant studies have confirmed that the combined deviation of resources and load will shift the capacity boundary [17]. Table 11 lists U0–U9. U1, where the solar power drops by 10%, raises the cost to 267.59 kUSD/year and the carbon emissions to 486.7 tCO2/year, has a greater impact than U3, where the wind speed drops by 10%. S4 is more sensitive to the deviation of solar power. U5 simultaneously reduces solar power and wind power by 10% and increases the agricultural load by 10%, and the LPSP remains at 0.0089. U6 and U8 enter the pressure feasible state, but do not cross the feasible boundary.

U8 represents the most unfavorable scenario. With a 20% decrease in solar irradiation, a 20% increase in agricultural load, and a 15% increase in electricity prices, the total annualized cost rises to 305.91 kUSD/year, carbon emissions reach 559.3 tCO2/year, PEE drops to 2.939 kg/kWh, and LPSP increases to 0.0108. This LPSP is still lower than 0.027 of the S1 scenario without energy storage. The buffer provided by energy storage and biomass did not fail under strong disturbances. On the contrary, U7 managed to reduce the cost to 236.42 kUSD/year when resources, load, and prices improved, and PEE rose to 3.353 kg/kWh. The redundant capacity did not lock in the beneficial returns of the system. Figure 8 plots carbon emissions and LPSP on the same coordinate. The two are generally in the same direction, but not completely linear. Electricity prices are

TABLE 10. Marginal Responses under a Positive 20% Parameter Shock

Parameter (+20% shock)	Cost response (%)	Carbon response (%)	PEE response (%)	LPSP after shock
PV capital cost	2.20	0.00	-0.19	0.0060
Battery capital cost	3.00	0.79	-0.59	0.0061
Grid electricity price	4.60	-1.00	0.40	0.0060
Grid emission factor	0.40	6.20	0.19	0.0060
Crop yield fluctuation	-0.20	0.00	11.61	0.0060
Agricultural load growth	3.60	2.61	-3.19	0.0061

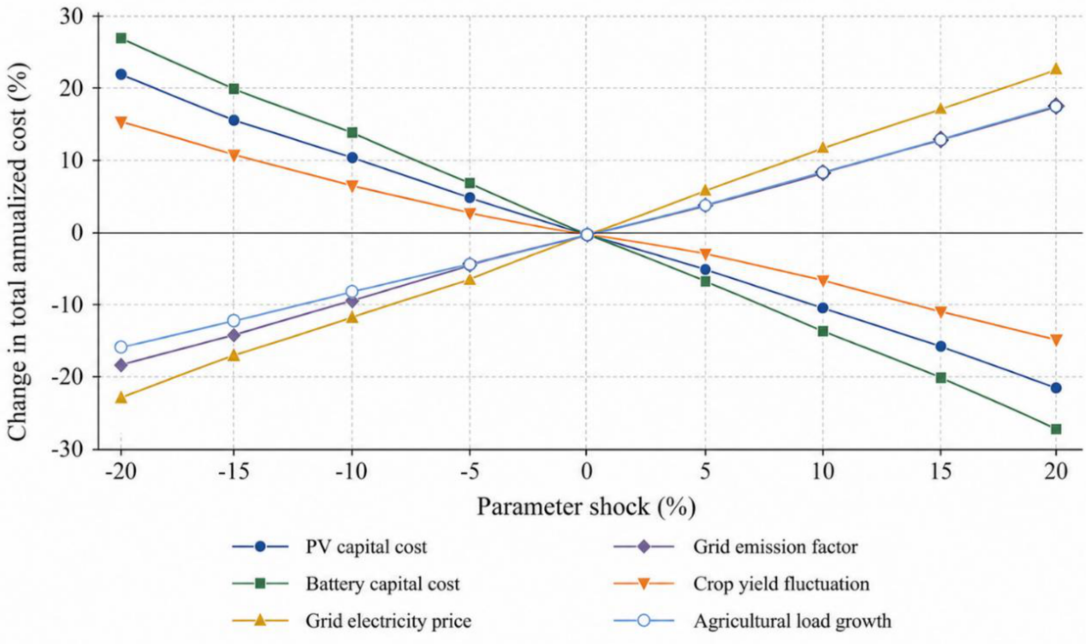

FIGURE 7. Sensitivity of Total Annualized Cost to Key Parameter Shocks

affected by the purchase cost, while resource and load deviations directly change the supply-demand gap. U6 and U8 both show high emissions and LPSP peaks simultaneously. All scenarios remain feasible or pressure-feasible, and H2 gains the second piece of evidence.

VI. DISCUSSION

A. COMPREHENSIVE JUDGMENT OF RESEARCH HYPOTHESES

H1 is supported by the obtained scenario, but the evidence chain does not directly jump from S0 to S4. S1 indicates that renewable energy can reduce costs and emissions, but it may damage reliability. S2 adds batteries, and LPSP and critical load guarantee rate recover. S3 and S4 then reduce unit output energy consumption through flexible scheduling and carbon constraints. The annual output increases from 842 to 858 t/year, and unit output energy consumption decreases from 426 to 310 kWh/t. Energy efficiency improvement comes from both energy saving and reduction of losses. H2 is supported by both capacity results and pressure scenarios. The battery handles daily fluctuations, and biomass covers the continuous low-resource periods; U8's LPSP is still significantly lower than S1. The reliability buffer comes from the complementary time scales of the two resources, not simply increasing redundancy. Biomass still has lifecycle emissions, so it is only suitable for undertaking guaranteed output. Whether hydrogen storage can replace this capacity remains to be determined when seasonal scale data and cost conditions are mature. H3 only holds within the existing scenarios. S2 to S3 introduce production flexibility, with a cost decrease of 6.13%, PEE increase of 6.42%, and renewable energy penetration rate increase by 4.9 percentage points. S3 to S4 simultaneously increase flexibility and tighten carbon constraints, and the cost change cannot be solely attributed to flexibility. Sensitivity results also show that time shifting cannot offset the growth in total energy demand. The existing evidence supports "time substitution with boundaries", but a continuous flexibility benefit curve cannot be given yet. H4 is supported by the consistency of multiple indicators. PEC-MOEA increases HV and the proportion of feasible solutions, IGD is also lower, and Spacing and Spread do not deteriorate. Hierarchical repair reduces the occupation of infeasible individuals by the computing budget. It also increases the running time. 142 s is still acceptable for the planning problem, but this advantage cannot be extrapolated to all multi-objective problems. The algorithm is effective

TABLE 11. Robustness under Renewable-Resource, Production-Load and Price Uncertainty

Case	Solar (%)	Wind (%)	Load (%)	Price (%)	TAC (kUSD/y)	CO2 (t/y)	LPSP	PEE	State
U0	0	0	0	0	259.80	468.0	0.0060	3.230	F
U1	-10	0	0	0	267.59	486.7	0.0069	3.182	F
U2	10	0	0	0	252.01	449	0.00	3.2	F
U3	0	-10	0	0	263.70	477.4	0.0065	3.204	F
U4	0	10	0	0	255.90	458.6	0.0055	3.256	F
U5	-10	-10	10	0	281.88	519.5	0.0089	3.059	F
U6	-15	-10	15	10	297.47	545.2	0.0101	2.986	SF
U7	10	10	-5	-10	236.42	423.5	0.0039	3.353	F
U8	-20	0	20	15	305.91	559.3	0.0108	2.939	SF
U9	0	-20	10	20	290.98	519.5	0.0085	3.081	F

Note: F = feasible; SF = stress-feasible.

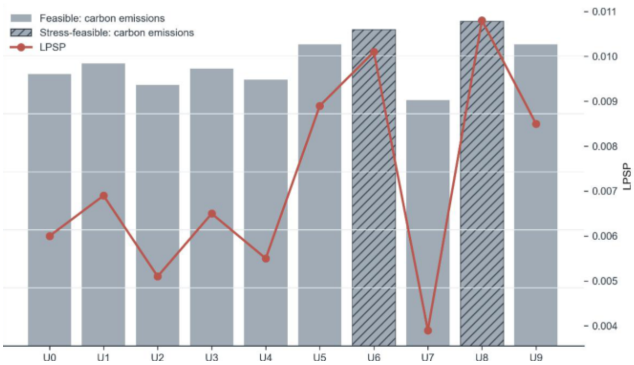

FIGURE 8. Carbon-Emission and Reliability Responses under Uncertainty Scenarios

because the repair sequence matches the consequences of agricultural default. Another alternative explanation still needs to be considered. The advantage of PEC-MOEA may mainly come from stronger feasibility repair rather than the evolutionary operators themselves. If the same repair rule is transplanted to NSGA-III or MOEA/D, the gap may be narrowed. The comparison of existing algorithms cannot yet separate these two contributions. Follow-up ablation experiments should fix the search operators and repair rules separately.

B. THEORETICAL CONTRIBUTIONS

The first change made by this paper is the evaluation object. Microgrid research usually leaves cost, emissions, and reliability at the energy level, while agricultural energy research often evaluates output after optimization. The agricultural-photovoltaic system has proved that energy benefits need to be examined together with crop responses [19]. This study directly writes production energy efficiency and critical load into the objectives and constraints. The evaluation problem no longer only asks how much energy can be supplied at a low cost, but also asks how much stable output these energies form. Reliability also has functional differences. The same power outage occurs in migratory irrigation periods and critical periods for cold chain, but the consequences are not the same. LPSP is suitable for comparing overall supply shortage, but it cannot hold the production bottom line. The critical load guarantee rate and hierarchical repair fill in this step. Aquaculture oxygen supply, livestock shed environmental control, and initial processing of agricultural products also have similar constraints, provided that the load function, allowable time windows, and default consequences can be identified. Load flexibility in this paper is a time choice right. It does not create energy, but only changes the time point when tasks occur. The benefit comes from the matching with low-carbon power sources, and the cost comes from environmental deviation and production risks. After the capacity and flexibility are encoded together, the adaptability of the production side is no longer an exogenous free resource. This also limits the improvement of digitalization in observability, but it does not automatically bring unlimited adjustability.

C. ENGINEERING DECISION AND POLICY IMPLICATIONS

S3 and S4 correspond to two business preferences. When the cash flow constraint is strong, the minimum annualized cost of S3 becomes more attractive. When taking on carbon targets or future carbon costs, S4 exchanges an incremental cost of 2.81% for an additional 24.52% reduction in emissions, while improving reliability and production energy efficiency. The park needs to select the solution from the Pareto set, and cannot consider a certain capacity combination as a long-term fixed answer. The energy storage control should obey the production priority, and cannot only follow the peak-valley electricity price. The biomass output should be reserved for low-resource and critical load periods. Migrable operations should be triggered by soil moisture, environmental conditions, and operation time windows. The purpose of the sensing system is to identify adjustable boundaries, not to expand the nominal flexibility. The planning model can be placed at the upper level, and the rolling control reprocesses minute and hour-level deviations. The subsidy for installed capacity will encourage the expansion of renewable energy, but does not guarantee production reliability. S1 is an example of the contrary. Support policies can simultaneously consider local consumption, available capacity of energy storage, critical load guarantee rate, and unit output carbon intensity. Biomass projects also need to verify the source of raw materials and lifecycle emissions. Regional shared energy storage should also retain the production bottom line of the single park, and cannot regard local shortages as an acceptable cost for system optimization. These indicators should not be directly transformed into unified assessment scores. The consequences of crop shortages vary greatly, and cold chain parks and open-field irrigation parks should not use the same reliability threshold. The policy end can stipulate the minimum data quality and accounting methods, and then the park can report the critical load set according to the crop system. This retains comparability and avoids replacing the risk judgment of the operating entity with a set of weights.

D. LIMITATIONS AND FURTHER RESEARCH

The research still has boundaries. The case comes from an anonymized park in the North China Plain, and other climate zones and crop systems need to be re-calibrated. Annual data is sorted by 15 minutes, and seasonal extreme processes still need to be analyzed separately. Battery degradation is replaced by annualized replacement cost, without explicitly simulating temperature, rate, and cycle depth. The existing scenarios do not have continuous scanning of the flexibility ratio, and the ablation experiment of the constraint repair module has not been completed. The next step should first supplement two types of evidence. The first is cross-seasonal and cross-crop meteorological-load-yield joint data to test the migrationability of capacity schemes. The second is the sequential operation of algorithms and module ablation to distinguish the contributions of critical load restoration, flexibility conservation, and trade-off selection.

VII. CONCLUSION

This paper incorporates agricultural production constraints into the capacity and scheduling decisions of microgrids and establishes a four-objective model and PEC-MOEA. The five progressive scenarios distinguish the roles of renewable energy access, energy storage configuration, production flexibility release, and carbon constraint tightening. The results do not support the simple judgment that "the more equipment installed, the more reliable". S1 reduced costs and emissions, but pushed the LPSP up to 0.027. S2 restored reliability after adding energy storage, S3 released load shift value when releasing load, and S4 continued to reduce emissions by 24.52% under a 2.81% increase in cost compared to S3. Compared to S0, the total annualized cost, carbon emissions, and unit output energy consumption of S4 decreased by 20.89%, 72.18%, and 27.23%, respectively, and production efficiency increased by 37.45%, and the critical load guarantee rate was 99.7%. The agricultural microgrid ultimately needs to answer not how many devices to install, but when to supply energy, which loads to protect first, and how much effective output these energies form. Energy storage and dispatchable biomass are responsible for cross-period buffering, agricultural flexibility is responsible for moving tasks within the agronomic boundaries, and constraint perception repair keeps infeasible solutions out of the Pareto comparison. All three links are indispensable.

REFERENCES

[1] X. Zhu, G. Ruan, H. Geng, and H. Liu, “Multi-Objective Sizing Optimization Method of Microgrid Considering Cost and Carbon Emissions,” IEEE Transactions on Industry Applications, 2024. DOI: 10.1109/TIA.2024.3395570.

[2] N. N. Ibrahim, J. J. Jamian, and M. M. Rasid, “Optimal multiobjective sizing of renewable energy sources and battery energy storage systems for formation of a multimicrogrid system considering diverse load patterns,” Energy, 2024. DOI: 10.1016/j.energy.2024.131921.

[3] C. Alvarez-Arroyo, S. Vergine, A. Sanchez De La Nieta, and L. Alvarado-Barrios, “Optimising microgrid energy management: Leveraging flexible storage systems and full integration of renewable energy sources,” Renewable Energy, 2024. DOI: 10.1016/j.renene.2024.120701.

[4] R. Banihabib, F. S. Fadnes, and M. Assadi, “Techno-economic optimization of microgrid operation with integration of renewable energy, hydrogen storage, and micro gas turbine,” Renewable Energy, 2024. DOI: 10.1016/j.renene.2024.121708.

[5] H. Dong, Y. Fu, Q. Jia, and T. Zhang, “Low carbon optimization of integrated energy microgrid based on life cycle analysis method and multi time scale energy storage,” Renewable Energy, 2023. DOI: 10.1016/j.renene.2023.02.034.

[6] V. V. Babu, J. P. Roselyn, and P. Sundaravadivel, “Multiobjective genetic algorithm based energy management system considering optimal utilization of grid and degradation of battery storage in microgrid,” Energy Reports, 2023. DOI: 10.1016/j.egyr.2023.05.067.

[7] P. N. D. Premadasa, C. M. M. R. S. Silva, D. P. Chandima, and J. P. Karunadasa, “A multi-objective optimization model for sizing an off-grid hybrid energy microgrid with optimal dispatching of a diesel generator,” Journal of Energy Storage, 2023. DOI: 10.1016/j.est.2023.107621.

[8] M. Rawa, Y. Al-Turki, K. Sedraoui, and S. Dadfar, “Optimal operation and stochastic scheduling of renewable energy of a microgrid with optimal sizing of battery energy storage considering cost reduction,” Journal of Energy Storage, 2023. DOI: 10.1016/j.est.2022.106475.

[9] S. Yadav, P. Kumar, and A. Kumar, “Optimal design and energy management in isolated renewable sources based microgrid considering excess energy and reliability aspects,” Journal of Energy Storage, 2024. DOI: 10.1016/j.est.2024.114320.

[10] Y. Wang, X. Guo, C. Zhang, and R. Liang, “Multi-strategy reference vector guided evolutionary algorithm and its application in multi-objective optimal scheduling of microgrid systems containing electric vehicles,” Journal of Energy Storage, 2024. DOI: 10.1016/j.est.2024.112500.

[11] K. Shafiei, A. Seifi, and M. Tarafdar Hagh, “A novel multiobjective optimization approach for resilience enhancement considering integrated energy systems with renewable energy, energy storage, energy sharing, and demand-side management,” Journal of Energy Storage, 2025. DOI: 10.1016/j.est.2025.115966.

[12] Y. Liu, Y. Tang, and C. Hua, “Multi-objective nutcracker optimization algorithm based on fast non-dominated sorting and elite strategy for grid-connected hybrid microgrid system scheduling,” Renewable Energy, 2025. DOI: 10.1016/j.renene.2025.122455.

[13] A. Rajendran and K. Selvam, “Multi-objective ChaoticEnhanced Competitive Swarm Optimizer algorithm based optimal scheduling of microgrid with renewable energy sources,” Energy, 2025. DOI: 10.1016/j.energy.2025.137550.

[14] Y. He and Y. Zhang, “Optimal configuration of shared energy storage for multi-microgrid systems: Integrating battery decommissioning value and renewable energy economic consumption,” Energy Conversion and Management, 2025. DOI: 10.1016/j.enconman.2025.120156.

[15] T. Hai, N. S. S. Singh, and F. Jamal, “Energy management of a microgrid with integration of renewable energy sources considering energy storage systems with electricity price,” Journal of Energy Storage, 2025. DOI: 10.1016/j.est.2024.115191.

[16] S. Jeon and S. Bae, “Integrated optimization for sizing, placement, and energy management of hybrid energy storage systems in renewable power systems,” Journal of Energy Storage, 2025. DOI: 10.1016/j.est.2024.114793.

[17] J. Wang, M. Aksoy, M. A. Rahman, and A. H. Alenezi, “Multi-objective planning and optimal configuration of wind, solar, and energy storage in inter-

connected microgrid clusters using Vine Copula scenario generation and antlion optimization," Renewable Energy, 2026. DOI: 10.1016/j.renene.2025.124313.

[18] F. D. Ferreira and R. Castro, "Multi-objective sizing and control of renewable energy communities with hybrid battery-hydrogen storage," Journal of Energy Storage, 2026. DOI: 10.1016/j.est.2026.122880.

[19] H. J. Williams, Y. Wang, B. Yuan, and M. I. Gomez, "Bringing solar to agriculture: An interdisciplinary design and analysis of a Concord grape agrivoltaic system," Applied Energy, 2025. DOI: 10.1016/j.apenergy.2025.126021.

[20] M. Temiz and I. Dincer, "Development of concentrated solar and agrivoltaic based system to generate water, food and energy with hydrogen for sustainable agriculture," Applied Energy, 2024. DOI: 10.1016/j.apenergy.2023.122539.

[21] S. Kim, S. Kim, and K. An, "An integrated multi-modeling framework to estimate potential rice and energy production under an agrivoltaic system," Computers and Electronics in Agriculture, 2023. DOI: 10.1016/j.compag.2023.108157.

[22] Y. Lu, C. L. Tan, Y. He, and F. Biljecki, "Multi-objective optimization of food, energy, and carbon for vertical agrivoltaic system on building facades," Energy and Buildings, 2025. DOI: 10.1016/j.enbuild.2025.116061.

[23] H. Ding, S. Tao, L. Zhang, and Y. Li, "Optimization Design of Agrivoltaic Systems Based on Light Environment Simulation," Agriculture, 2025. DOI: 10.3390/agriculture15232437.

[24] N. Chowdhury, M. Calais, and G. M. Shafiullah, "Optimization approaches for renewable microgrid applications with hydrogen and battery energy storage: A comprehensive review," Journal of Energy Storage, 2026. DOI: 10.1016/j.est.2026.122744.

[25] R. Yasmin, M. N. Nabi, A. K. Azad, and M. A. Hossain, "Recent advances in low-carbon hydrogen: Production, storage, and DC microgrid energy management under uncertainty," Renewable and Sustainable Energy Reviews, 2026. DOI: 10.1016/j.rser.2026.117229.